JACS
JOURNAL OF THE AMERICAN CHEMICAL SOCIETY

Subscriber access provided by American Chemical Society

Communication

Single-Crystalline Vanadium Dioxide Nanowires with Rectangular Cross Sections

Beth S. Guiton, Qian Gu, Amy L. Prieto, Mark S. Gudiksen, and Hongkun Park

J. Am. Chem. Soc., **2005**, 127 (2), 498-499• DOI: 10.1021/ja045976g • Publication Date (Web): 23 December 2004

Downloaded from http://pubs.acs.org on March 24, 2009

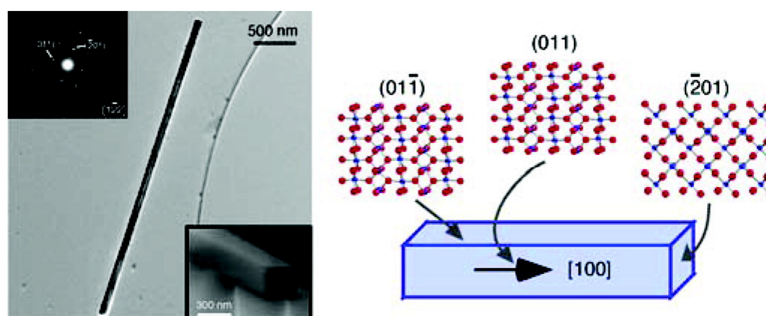

More About This Article

Additional resources and features associated with this article are available within the HTML version:

- Supporting Information
- Links to the 18 articles that cite this article, as of the time of this article download
- Access to high resolution figures
- Links to articles and content related to this article
- Copyright permission to reproduce figures and/or text from this article

View the Full Text HTML

ACS Publications
High quality. High impact.

Journal of the American Chemical Society is published by the American Chemical Society. 1155 Sixteenth Street N.W., Washington, DC 20036

J|A|C|S
COMMUNICATIONS

Published on Web 12/23/2004

Single-Crystalline Vanadium Dioxide Nanowires with Rectangular Cross Sections

Beth S. Guiton, Qian Gu, Amy L. Prieto, Mark S. Gudiksen, and Hongkun Park*

Department of Chemistry and Chemical Biology, Harvard University, 12 Oxford Street, Cambridge, Massachusetts 02138

Received July 6, 2004; E-mail: hpark@chemistry.harvard.edu

Nanometer-sized materials often exhibit physical and chemical properties that differ greatly from their bulk counterparts.[1] One-dimensional nanostructures,[2,3] such as nanotubes, nanorods, and nanowires, represent a particularly attractive class of materials because they exhibit many novel characteristics owing to their small radial dimension while retaining wirelike connectivity. Although earlier synthetic efforts have been directed mostly toward carbon nanotubes[2] and semiconductor[3,4] and metallic[5,6] nanowires, synthetic methods for transition-metal oxides are also beginning to emerge.[7−15]

Vanadium dioxide (VO_2) undergoes a Mott metal−insulator transition (MIT) close to room temperature[16] and has been suggested as a candidate for realizing electrically driven Mott field-effect transistors (FETs).[17,18] The MIT in VO_2 is characterized by an abrupt change in resistivity (by a factor of 10^4-10^5) at $T_C = 340$ K.[16] Accompanying this MIT is a small structural distortion of the underlying VO_2 lattice from a low-temperature monoclinic (semiconducting phase) to a high-temperature tetragonal rutile (metallic phase) structure. Previous work on nanoscale VO_2 has utilized nanoparticles[19,20] and thin films[17,18,21] to study the finite-size effects of the Mott MIT[19−21] and the fabrication of Mott FETs.[17,18] Attempts to synthesize nanoscale VO_2 with wirelike morphologies have yielded only polycrystalline nanorods.[11,22]

Here we report the synthesis and characterization of single-crystalline, well-faceted VO_2 nanowires with rectangular cross sections. The synthesis was performed using a vapor transport method:[13] bulk VO_2 powders were placed in a quartz boat in the center of a horizontal tube furnace, and temperature (T), pressure (P), evaporation time (t), and argon carrier gas flow rate (k_{flow}) were controlled to obtain the desired product. The reaction product was collected on a substrate downstream from the starting material. Optimum reaction conditions resulting in the growth of VO_2 nanowires were $T = 900-1100$ °C, $P = 12-13$ Torr, $t = 5$ h, and $k_{flow} \approx 3$ sccm. The reliable production of nanowires required a careful choice of substrate surface; the greatest nanowire density was achieved when a Si_3N_4 substrate was used, whereas SiO_2 substrates produced extremely low densities of long wires.

The morphology of the reaction product was examined using scanning electron microscopy (SEM) and transmission electron microscopy (TEM). Figure 1a shows a representative SEM image and illustrates that the reaction produces predominantly straight nanowires with well-defined facets. Cross-sectional SEM images, such as that shown in the Figure 1a inset (see also Supporting Information), have further revealed that these nanowires exhibit clear rectangular cross sections. Imaging of the reaction products from multiple reaction runs shows that the average width of a typical VO_2 nanowire is 60 (±30) nm with lengths reaching up to >10 μm when the optimum reaction conditions are used. The dimensions of nanowires were sensitively dependent on the reaction conditions, however, and reactions performed at higher temperature, lower pressure, and for longer reaction time yielded thicker nanowires with high wire density (see Figures S1 and S4 in Supporting Information).

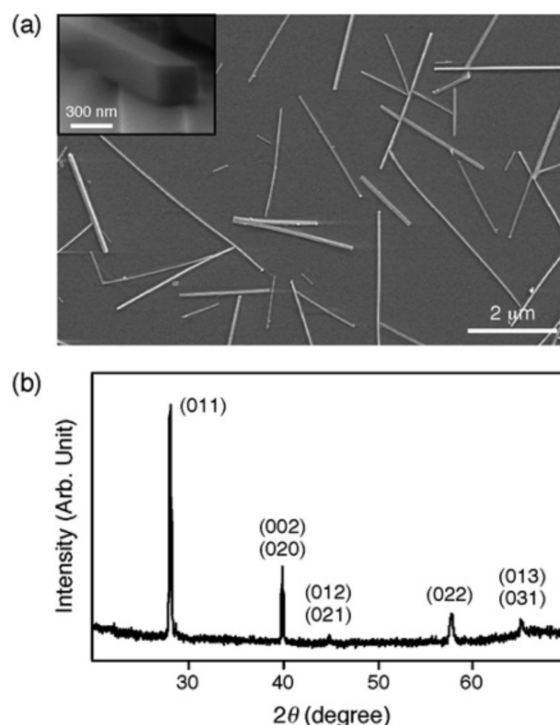

Figure 1. (a) SEM image of VO_2 nanowires as grown on a Si_3N_4 substrate. The reaction conditions were $T = 900$ °C, $P \approx 12$ Torr, $t = 5$ h, and $k_{flow} \approx 3$ sccm. Inset: cross-sectional SEM image showing the rectangular cross section of a VO_2 nanowire. (b) X-ray diffraction pattern of as-synthesized VO_2 nanowires.

The structure of the VO_2 nanowires was examined using X-ray diffraction (XRD) and TEM. Figure 1b shows a representative XRD pattern of an as-synthesized sample and demonstrates clearly that the nanowire products are highly crystalline. The XRD peaks can be indexed unambiguously to the low-temperature, monoclinic form of VO_2 (JCPDS file 72-0514; see Figure S5 in Supporting Information). The most striking feature in Figure 1b is the absence of all peaks other than those belonging to the (0*kl*) family, which strongly suggests that the VO_2 nanowires have a preferential growth direction.

Figure 2a shows a TEM image of a representative VO_2 nanowire and a selected area electron diffraction (SAED) pattern obtained from the same nanowire. To make TEM samples, nanowires were released from the nitride surface by sonicating the as-grown sample in 4 M KOH, followed by neutralization with HNO_3 and deposition of the nanowire solution onto a TEM grid. The SAED pattern is indexed to monoclinic VO_2, with a zone axis of $[1\bar{2}2]$. Significantly, the diffraction pattern did not change as the electron beam was

10.1021/ja045976g CCC: $30.25 © 2005 American Chemical Society

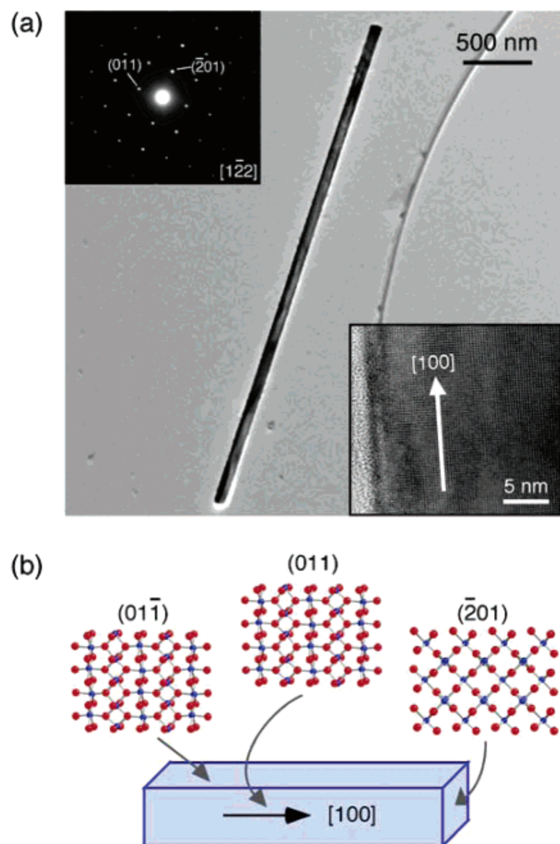

Figure 2. (a) TEM image of a VO_2 nanowire. Upper inset: SAED pattern indexed for monoclinic VO_2 on the $[1\bar{2}2]$ zone axis. Lower inset: High-resolution TEM image of a VO_2 nanowire. (b) Schematic of a VO_2 nanowire with the bounding surfaces indicated. Blue indicates V atoms, and the red indicates O atoms.

moved along the nanowire, indicating that the whole nanowire is a single crystal. The lower inset to Figure 2a shows a high-resolution TEM image of a nanowire with clear lattice fringes, again confirming its high crystallinity. Careful analysis of the SAED patterns from multiple nanowires showed that the nanowires are single crystalline with an axial growth plane of $(\bar{2}01)$ and, accordingly, a growth axis in the [100] direction. This growth direction is fully consistent with the exclusive presence of the (0*kl*) peaks in Figure 1b, demonstrating that most, if not all, nanowires grow along the [100] direction.

Both SEM and TEM images revealed that approximately 2% of the reaction products exhibit a “bent-wire” morphology. This bending arises from the formation of a twin boundary at the {100} planes, which causes an abrupt 115° change in direction of the wire. Electron microscope images and diffraction data show that, like the straight wires, each branch of these twinned wires also grows along the [100] direction (see Figure S3 in Supporting Information).

The SAED pattern in Figure 2a, combined with the rectangular cross section shown in Figure 1a, allows the unambiguous determination of the bounding facet indices of the VO_2 nanowires. Specifically, the top facet of the nanowire in Figure 2a, which is perpendicular to the electron beam, is $(01\bar{1})$. The crystallographic symmetry of monoclinic VO_2 then dictates that the side facet bounding the same nanowire should be (011), as illustrated in Figure 2b. This conclusion is supported by the SAED patterns of all nanowires investigated to date. The bounding $(01\bar{1})$ and (011) facets are crystallographically equivalent, low-index, and therefore, low-energy surfaces. This observation explains the rectangular cross sections of the VO_2 nanowires as well as their unique growth direction. The strong dependence of nanowire growth on the substrate type suggests that the Si_3N_4 layer provides a seeding environment for nanowire growth. Though the exact growth mechanism is still unknown, we suggest that a likely model is a diffusion-based vapor-solid mechanism, as proposed by Dai et al.[13] The interplay between the surface energetics and the substrate effect requires further investigation.

The single-crystalline VO_2 nanowires reported here present a new model system for the investigation of the Mott MIT in nanoscale VO_2. These nanowires may also allow the fabrication of nanometer-scale Mott FET devices.

Acknowledgment. This work was supported by the NSF Career Award and the Harvard NSEC Award. We thank M. Deshmukh, D. Lange, D. Bell, W. MoberlyChan, Y. Lu, J. Tsakirgis, and M. Biercuk for discussions and technical assistance.

Note Added in Proof. The synthesis of metastable VO_2 nanobelts was recently reported by Liu et al.[23]

Supporting Information Available: Further SEM, TEM and SAED data, histograms of nanowire widths, XRD simulations, energy-dispersive X-ray spectroscopy data, and X-ray photoelectron spectroscopy data. This material is available free of charge via the Internet at http://pubs.acs.org.

References

(1) Alivisatos, A. P. *Science* **1996**, *271*, 933−937.
(2) Odom, T. W.; Huang, J.-L.; Kim, P.; Lieber, C. M. *J. Phys. Chem. B* **2000**, *104*, 2794−2809.
(3) Hu, J.; Odom, T. W.; Lieber, C. M. *Acc. Chem. Res*. **1999**, *32*, 435−445.
(4) Peng, X.; Manna, L.; Yang, W.; Wickham, J.; Sher, E.; Kadavanich, A.; Alivisatos, A. P. *Nature* **2000**, *404*, 59−61.
(5) Puntes, V. F.; Krishnan, K. M.; Alivisatos, A. P. *Science* **2001**, *291*, 2115−2117.
(6) Wang, J.; Tian, M.; Mallouk, T. E.; Chan, M. H. W. *J. Phys. Chem. B* **2004**, *108*, 841−845.
(7) Satishkumar, B. C.; Govindaraj, A.; Nath, M.; Rao, C. N. R. *J. Mater. Chem.* **2000**, *10*, 2115−2119.
(8) Pan, Z. W.; Dai, Z. R.; Wang, Z. L. *Science* **2001**, *291*, 1947−1949.
(9) Huang, M. H.; Wu, Y.; Feick, H.; Tran, N.; Weber, E.; Yang, P. *Adv. Mater.* **2001**, *13*, 113−116.
(10) Urban, J. J.; Yun, W. S.; Gu, Q.; Park, H. *J. Am. Chem. Soc.* **2002**, *124*, 1186−1187.
(11) Patzke, G. R.; Krumeich, F.; Nesper, R. *Angew. Chem., Int. Ed.* **2002**, *41*, 2446−2461.
(12) Yang, P.; Yang, H.; Mao, S.; Russo, R.; Johnson, J.; Saykally, R.; Morris, N.; Pham, J.; He, R.; Choi, H.-J. *Adv. Funct. Mater.* **2002**, *12*, 323−331.
(13) Dai, Z. R.; Pan, Z. W.; Wang, Z. L. *Adv. Funct. Mater.* **2003**, *13*, 9−24.
(14) Cozzoli, P. D.; Kornowski, A.; Weller, H. *J. Am. Chem. Soc*. **2003**, *125*, 14539−14548.
(15) Cheng, B.; Russell, J. M.; Shi, W.; Zhang, L.; Samulski, E. T. *J. Am. Chem. Soc.* **2004**, *126*, 5972−5973.
(16) Morin, F. J. *Phys. Rev. Lett.* **1959**, *3*, 34−36.
(17) Chudnovskiy, F.; Luryi, S.; Spivak, B. In *Future Trends in Microelectronics: the Nano Millenium*; Zaslavsky, A., Ed.; Wiley-Interscience: New York, 2002; pp 148−155.
(18) Kim, H.-T.; Chae, B.-G.; Youn, D.-H.; Maeng, S.-L.; Kim, G.; Kang, K.-Y.; Lim, Y.-S. *New J. Phys.* **2004**, *6*, 52 51−19.
(19) Lopez, R.; Boatner, L. A.; Haynes, T. E.; Feldman, L. C.; Haglund, R. F., Jr. *J. Appl. Phys.* **2002**, *92*, 4031−4036.
(20) Lopez, R.; Haynes, T. E.; Boatner, L. A.; Feldman, L. C.; Haglund, R. F., Jr. *Phys. Rev. B* **2002**, *65*, 224113.
(21) Kim, H. K.; You, H.; Chiarello, R. P.; Chang, H. L. M.; Zhang, T. J.; Lam, D. J. *Phys. Rev. B* **1993**, *47*, 12900−12907.
(22) Gui, Z.; Gan, R.; Mo, W.; Chen, X.; Yang, L.; Zhang, S.; Hu, Y.; Wang, Z.; Fan, W. *Chem. Mater.* **2002**, *14*, 5053−5056.
(23) Liu, J.; Li, Q.; Wang, T.; Yu, D.; Li, Y. *Angew. Chem., Int. Ed.* **2004**, *43*, 5048−5052.

JA045976G